AD NUMBER: AD0482927

LIMITATION CHANGES

TO:

Approved for public release; distribution is unlimited.

FROM:

Distribution authorized to US Government Agencies and their Contractors; Administrative/Operational Use; 1 Mar 1961. Other requests shall be referred to US Army Electronics Command, Army Signal Supply Agency, Fort Monmouth, NJ 07703.

AUTHORITY

USAEC ltr dtd 27 Jul 1971

Technical Memorandum

IONIZATION BELOW 100 KM DUE TO RADIOACTIVE CLOUDS

Prepared for:

UNITED STATES ARMY SIGNAL SUPPLY AGENCY
FORT MONMOUTH PROCUREMENT OFFICE
FORT MONMOUTH, NEW JERSEY

CONTRACT DA 36-039 SC-85119

By: *E. T. Pierce*

STANFORD RESEARCH INSTITUTE

MENLO PARK, CALIFORNIA

STANFORD RESEARCH INSTITUTE
MENLO PARK, CALIFORNIA

March 1961

Technical Memorandum

IONIZATION BELOW 100 KM DUE TO RADIOACTIVE CLOUDS

Prepared for:

UNITED STATES ARMY SIGNAL SUPPLY AGENCY
FORT MONMOUTH PROCUREMENT OFFICE
FORT MONMOUTH, NEW JERSEY

CONTRACT DA 36-039 SC-85119

By: *E. T. Pierce*

SRI Project No. 3097

Approved:

A M Peterson (WER)

A. M. PETERSON, MANAGER COMMUNICATION AND PROPAGATION LABORATORY

Copy No. 6

ABSTRACT

The ionization produced by radioactive clouds located in the stratosphere is examined. As an example, a cloud of 3×10^{12} curies activity centered at 30 km height and emitting 1 Mev β and γ radiation is considered. Contours for the rate of electron production are derived and converted into contours of equal electron density using appropriate values for detachment, attachment, and recombination coefficients. Immediately above the cloud, electron densities exceeding 10^5 (cm^{-3}) are found for heights up to 75 km; there is also a lateral spread of the contours which is most pronounced at 70 km. The effects in absorption upon a frequency of 18 Mc are deduced. It is also shown that at night the width—usually 90 km—of the waveguide controlling VLF propagation is reduced over a horizontal distance of 400 km to a minimum of only 30 km.

CONTENTS

ILLUSTRATIONS

IONIZATION BELOW 100 KM DUE TO RADIOACTIVE CLOUDS

I INTRODUCTION

A nuclear explosion at the instant of detonation releases large quantities of energetic particles and electromagnetic radiation capable of producing ionization in the atmosphere. However, in addition to these immediate sources of ionization, the radioactive products generated by the explosion represent a continuing ionizing source. This note is concerned with the ionization due to these products. Following the explosion the radioactive material is concentrated within a cloud whose dimensions increase steadily, while the total activity decreases. This behavior is illustrated in Table I.

Table I

SIZE OF EXPLOSION		TIME AFTER EXPLOSION			
		Minute	Hour	Day	Week
20 kT	Total Radioactivity (curies)	10^{12}	6×10^{9}	10^{8}	10^{7}
	Radius of cloud (km)	0.6	4	35	90
20 MeT	Total Radioactivity (curies)	10^{15}	6×10^{12}	10^{11}	10^{10}
	Radius of cloud (km)	1.5	10	40	90

The figures in Table I are derived from an obscure unclassified paper,[1] but other unclassified information[2,3] is in agreement with Table I.

Table I represents a guide to the quantity of radioactivity and the dimensions of the cloud associated with an explosion of known yield One additional important factor is the height at which the cloud is centered. It appears[4,5] that kiloton weapons, when detonated in the troposphere, produce radioactive clouds that do not extend above the tropopause. On the other hand, the fireballs due to explosions with yields in the megaton class do not stabilize before reaching the lower or intermediate stratosphere. For instance, the upper limit of the cloud due to a megaton explosion has been quoted[6] as being at 25 km.

It is far beyond the scope of this note to attempt to cover the situations resulting from all appropriate nuclear explosions and for all

times following the explosion. Indeed the main purpose of the succeeding analysis is merely to demonstrate that a persistent radioactive cloud in the stratosphere can produce appreciable ionization of equal persistence at heights of up to at least 100 km. It is felt that this demonstration can best be achieved by examining a specific example in some detail. A radioactive cloud of total activity 3×10^{12} curies will be considered; this, from Table I is the activity to be expected one hour after a 10-MeT explosion. The cloud will be taken as spherical and of 10-km radius, since Table I indicates that the cloud dimensions depend very little upon the size of an explosion. Any distortion of the cloud, such as probably results from winds and other factors, will be ignored. The cloud is assumed to be centered at a height of 30 km.

It is thought that the example selected is a good illustration of some of the problems involved, and that the analysis developed can obviously be applied to other particular cases.

II THE RADIOACTIVE PRODUCTS

Most radioactive products decay by the emission of a β particle or of γ radiation or of both; α disintegration is relatively rare. Accordingly, it seems reasonable to neglect α emission and assume that only β and γ activity is involved. Both the β and γ emissions will cover a very large range in energies since many different radioactive isotopes will be present. However, to take account of this spectral distribution would entail almost intolerable complexities. Accordingly it will be assumed that the emissions are monoenergetic, and a good averaging compromise is to take each radioactive disintegration as being responsible for a β particle and a γ quantum both of 1-Mev energy.

III THE β EMISSION

The specific example to be considered has a cloud of radius 10 km centered at a height of 30 km; thus the maximum height of the edge of the cloud is 40 km and the minimum 20 km. β particle ranges are usually given in aluminum; it seems reasonable, however, to take an inverse proportionality with the density, ρ, of the medium, in which case the range, R, may be expressed as

$$R = \frac{(542\ E - 133)}{1000\rho}\ cm \qquad (1)$$

where E is in Mev and ρ in g cm^{-3}. Equation (1) yields 12.2 meters as the range of a 3-Mev β particle in air at sea level; this figure is in reasonable agreement with the 13 meters quoted in the Smithsonian Physical Tables.[7] Using the figures for air density available in the ARDC model atmosphere,[8] Eq. (1) gives the range of a 1-Mev β-particle at heights of 20, 30, and 40 km, to be approximately 45, 230, and 1000 meters, respectively. Thus, even at the greatest altitude attained by the cloud, the ionization produced by the β radiation extends only about a kilometer beyond the boundary of the cloud. Hence it is an assumption, not greatly in error, to take the β-produced ionization as being spatially coincident with the radioactive cloud.

At energies less than a few Mev, β particles traveling in an absorbing medium lose energy principally by ionization and excitation of the atoms of the absorber; radiation or bremsstrahlung losses are small. Most textbooks state that for a β particle travelling in air the particle loses some 32 ev in energy for each ion-pair created; the total number of ion-pairs produced by a 1-Mev β particle would therefore be approximately 3.2×10^4.

Within the radioactive cloud the ion production due to the β rays will be essentially uniform. The variation of range with air density implies that fewer βs will pass through unit volume near the base of the cloud than will be the case for higher in the cloud; on the other hand, the shorter ranges mean more ions produced per unit length of path. These two competing influences lead to a mutual balance. If q_β is the number of electrons produced (cm^{-3} sec^{-1}) then

$$q_\beta = \frac{\left(\begin{array}{c}\text{Total } \beta \text{ activity} \\ \text{in curies}\end{array}\right)\left(\begin{array}{c}\text{Number of disintegrations} \\ \text{per sec per curie}\end{array}\right)\left(\begin{array}{c}\text{Total ionization} \\ \text{per each } \beta\end{array}\right)}{(\text{Volume of cloud})}$$

$$= \frac{(3 \times 10^{12})(3.7 \times 10^{10})(3.2 \times 10^{4})}{1.33 \times \pi \times 10^{3} \times 10^{15}} \qquad (2)$$

$$= 8.5 \times 10^{8} \ (\text{cm}^{-3} \ \text{sec}^{-1})$$

for the particular case being considered.

IV THE γ EMISSION

γ rays are much more penetrating than β particles and it would be a gross error to take the γ produced ionization as being even approximately coincident with the radioactive cloud. The absorption of γ rays within a homogeneous medium follows the exponential law

$$I_x = I_0 \exp(-\rho\mu_m x) \tag{3}$$

where I_0 is the initial flux and I_x the flux after traveling a distance x in the medium. ρ is the density and μ_m the mass absorption coefficient; for air and γ rays of 1-Mev energy, $\mu_m = 0.063$ cm^2/gm.[9] For γ rays in the atmosphere, ρ will, in general, vary with x except for the case of horizontal attenuation. It is not difficult to take account of this factor, by simply noting that $-\rho x = M_x$, the mass of the column of air of unit cross section and length x, and can therefore be expressed in terms of pressures. For the simple case of vertical attenuation where h is the height coordinate,

$$I_h = I_0 \exp\left(-\mu_m \int_0^h \rho dh\right) .$$

Using the hydrostatic equation $dp/dh = -g\rho$, where p is the pressure and g the acceleration due to gravity, yields

$$I_h = I_0 \exp\left[\frac{\mu_m}{g}(p_h - p_0)\right] . \tag{4}$$

Strictly speaking, an error is involved in assuming that g is constant, since actually g varies with h, but the error is only slight. For the case where the γ ray flux is generated by a cloud at a height H, the zero is at $h = H$ and Eq. (4) becomes

$$I_h = I_H \exp\left[\frac{\mu_m}{g}(p_h - p_H)\right]$$

$$I_h = I_H \exp [0.065 (p_h - p_H)] \qquad (5)$$

where the pressures are measured in millibars (10^3 dynes cm^{-2}). It is interesting to note that for the particular example being considered (H = 30 km, p_{30} = 11.9 mb) then with $h = \infty (p_h = 0)$, $I_h/I_H = \exp [0.065 (-11.9)] \approx 0.46$; that is, nearly half the vertically directed γ flux escapes into space without any effect upon the atmosphere. If the height is lowered to 20 km (p_{20} = 55.3 mb), the confinement within the atmosphere is much more efficient and only some 3 percent of the vertical γ flux escapes.

The most important initial process in the absorption of γ rays of 1-Mev energy is the Compton effect; the incident γ photon transfers its energy to a Compton electron and to a photon of less energy than the original γ. In turn, the second photon may participate in further Compton processes until the photon energy is eventually reduced to a value readily absorbed by photoelectric ejection of an orbital electron from an atom. Thus the γ ray energy is converted into energy of Compton and photo electrons. These, in turn, lose energy by ionization in a manner entirely similar to that of the β radiation. It will be taken, as in Sec. III, that 3.2×10^4 ion-pairs are produced for each photon of 1-Mev γ radiation that is absorbed.

Since the γ rays, particularly those having an upwardly directed velocity component, penetrate to distances far greater than the dimensions of the radioactive cloud, it is not a gross error to assume that the source is effectively a point source concentrated at the center of the cloud. Because this assumption leads to a very considerable analytical simplification, it will be adopted in the analysis that follows.

ELECTRON PRODUCTION BY THE γ EMISSION

Suppose the cloud is centered at point 0 ($h = H$). Consider the ionization produced at a point $B(h = H + z)$ where the line $OB(=l)$ makes an angle θ with the upward vertical through 0. Then it follows that the attenuation along OB is proportional to

$$\exp (-\mu_a M_{OB}) = \exp \left[- \frac{\mu_a \sec \theta}{g} (p_H - p_{H+z}) \right] . \qquad (6)$$

If I_B is the flux incident per cm^2 at B along OB, and I_0 would have been the corresponding flux without any attenuation along OB,

$$I_B = I_0 \exp\left(-\frac{\mu_m \sec\theta}{g} p_H\right) \exp\left(+\frac{\mu_m \sec\theta}{g} p_{H+z}\right) \quad . \qquad (7)$$

Consider unit volume at B, the volume being formed of a conical frustum with apex at O, bounded by planes equidistant from B and normal to OB, and of unit cross-sectional area at B. Then the absorption of the γ radiation within this volume is given by

$$\frac{dI_B}{dl} = \frac{1}{\sec\theta} \cdot \frac{dI_B}{dz} = \frac{1}{\sec\theta} \cdot I_B \frac{\mu_m \sec\theta}{g} \frac{dp_{H+z}}{dz}$$

$$= -\mu_m \rho_{H+z} I_B \qquad (8)$$

and this is the energy that is converted into ionization.

Suppose the magnitude of the source at O is C curies. Then allowing for the radial divergence of flux

$$I_0 = \frac{3.7 \times 10^{10}}{4\pi l^2} \cdot C = \frac{3.7 \times 10^{10}}{4\pi z^2 \sec^2\theta} \cdot C \quad . \qquad (9)$$

As before, it may be taken that each photon of 1-Mev γ radiation that is absorbed produces 32×10^3 ion-pairs; furthermore, for the particular example, $C = 3 \times 10^{12}$ curies. Combining Eqs. (7),(8), and (9), q_B, the rate of electron production (cm^{-2} sec^{-1}) due to the γ radiation, may be written as

$$q_B = 32 \times 10^3 \left(\frac{dI_B}{dl}\right)$$

$$= 32 \times 10^3 (\mu_m \rho_{H+z}) \frac{3.7 \times 10^{10} \times 3 \times 10^{12}}{4\pi z^2 \sec^2\theta} \exp\left[\frac{\mu_m \sec\theta}{g} (p_{H+z} - p_H)\right]$$

$$= 1.78 \times 10^{15} \frac{\rho_{H+z}}{z^2 \sec^2\theta} \exp[0.065\, p_{H+z} \sec\theta] \exp[-0\ 065 p_H \sec\theta] \qquad (10)$$

where the pressures are measured in millibars and z is in kilometers, while ρ is in gram cm^{-3}. Often ρ is tabulated in kg m^{-3}; if so,

$$q_B = 1.78 \times 10^{12}\left(\frac{\rho_{H+z}}{z^2 \sec^2\theta}\right) \exp\{0.065\ p_{H+z} \sec\theta\} \exp\{-0.065 p_H \sec\theta\} \tag{11i}$$

Both Eqs. (10) and (11) are in a suitable form for calculation, the most convenient procedure for a given H being to select a value of θ and then calculate q_B for a series of values of z, the pressures and densities being obtained from Ref. 8; the procedure is then repeated for another θ.

V THE ELECTRON BALANCE EQUATIONS

Figure 1 shows the results obtained when Eq. (11) for q_B is evaluated It may be noted that for heights less than H Eq. (11) modifies to

$$q_B = 1.78 \times 10^{12} \left(\frac{\rho_{H-Z}}{Z^2 \sec^2 \theta} \right) \exp \{-0.065\ p_{H-Z} \sec \theta\} \exp \{+0.065\ p_H \sec \theta\} \tag{11a}$$

where Z is the vertical co-ordinate measured downward from $h = H$ as origin.

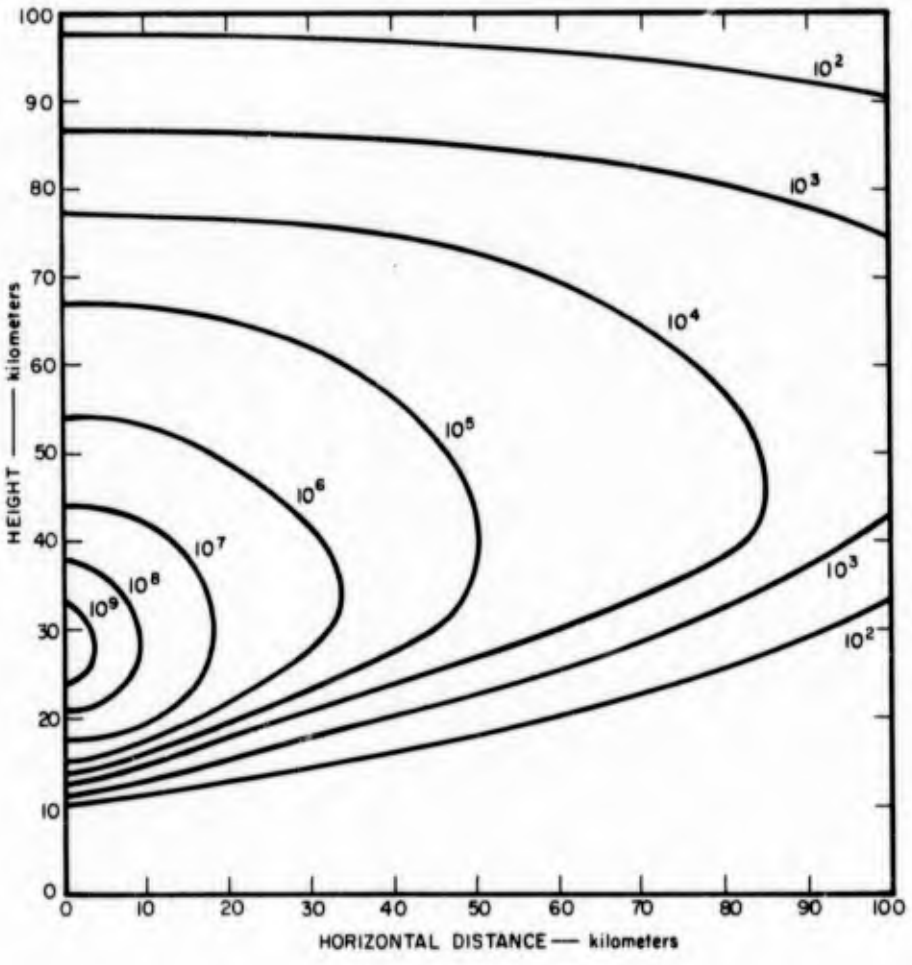

FIG. 1

CONTOURS OF ELECTRON PRODUCTION ($cm^{-3}\ sec^{-1}$) DUE TO γ RADIATION

A height range of from zero to 100 km and a lateral extent of 100 km from the center of the cloud are covered, flat-earth conditions being taken. Figure 1 is effectively half of a vertical cross section through the center of the cloud and the more adjacent atmosphere. The symmetry of the situation obviously means that the contours of q_B, shown in Fig. 1, could be converted into the true surfaces of revolution representing equal values of q_B by rotation around the vertical axis at zero horizontal distance.

In order to convert the information for q_B into contours of electron density, it is necessary to take account of the electron and negative ion balance equations. These are complicated and must be simplified considerably before any tractable relations are obtained. Not all the information necessary for the simplification processes is available; in consequence, the procedure involves the making of plausible assumptions.

Taking electrical neutrality as being always present everywhere in the atmosphere, so that the concentration of positive ions is equal to the sum of the number of electrons per unit volume N_e and of the concentration N_- of negative ions, the two balance equations may be written in the form

$$\frac{dN_e}{dt} = q + N_- d + N_- \sigma N - N_e(N\beta' + N^2\tau) - (N_- + N_e)\{N_e\alpha' + N_e N\alpha'' + N_e\alpha'''\} \tag{12}$$

for electrons and

$$\frac{dN_-}{dt} = -N_- d - N_- \sigma N + N_e(N\beta' + N^2\tau) - (N_- + N_e)(N_-)\{\gamma' + N\epsilon\} \tag{13}$$

for ions. In Eqs. (12) and (13) N is the density of neutral particles. Assuming equilibrium conditions,

$$\frac{dN_e}{dt} = 0 = \frac{dN_-}{dt} .$$

Considering the terms in the equations in detail, q is the rate of production of electrons (cm^{-3} sec^{-1}). The succeeding term in Eq. (12) represents photodetachment, by incoming solar radiation, of negative ions to form electrons; a simplification that will be applied is to take night conditions under which $d = 0$. The next term in Eq. (12) represents

collisional detachment of negative ions to form electrons. The fourth term is the attachment of electrons to become negative ions; two attachment processes are recognized, namely radiative attachment (coefficient β') and the Bloch-Bradbury three-body process (coefficient τ). The final term in Eq. (12) indicates the loss of electrons by recombination with positive ions; the three coefficients refer, respectively, to dissociative recombination, three-body recombination, and radiative recombination. The indications are that $\alpha''' << \alpha'$ and can therefore be neglected. The first three terms of Eq. (13) have already been considered, and the fourth represents recombination between positive and negative ions; the two coefficients refer, respectively, to two-body ion recombination and three-body Thompson ion recombination. In passing, it may be stated that although Eqs. (12) and (13) are fairly complicated they in fact incorporate simplifications which are to some extent misleading. For instance, the the term $N^2\tau$ is not the same for all neutral constituents of the atmosphere, molecular oxygen being much more effective than molecular nitrogen as the third body in a collisional attachment process. Similar refinements apply to many of the other terms.

When account is taken of the remarks in the preceding paragraph Eqs. (12) and (13) reduce to

$$q + N_- \sigma N - N_e(N\beta' + N^2\tau) - (N_- + N_e)(N_e)\{\alpha' + N\alpha''\} = 0 \qquad (14)$$

$$- N_- \sigma N + N_e(N\beta' + N^2\tau) - (N_- + N_e)(N_-)\{\gamma' + N\epsilon\} = 0 \qquad (15)$$

and these equations may be rewritten as

$$q + KN_- - \eta N_e - \alpha N_e(N_- + N_e) = 0 \qquad (16)$$

$$- KN_- + \eta N_e - \gamma N_-(N_- + N_e) = 0 \ . \qquad (17)$$

Equations (16) and (17) may be combined to yield

$$N_e = \left[\frac{q}{(1+\lambda)(\alpha + \lambda)}\right]^{1/2} \qquad (18)$$

where $\lambda = N_-/N_e$, the ratio of negative ion and electron densities, and Eq. (18) may for convenience be modified to

$$N_e = \left(\frac{q}{\beta}\right)^{1/2}$$
$$\beta = (1 + \lambda)(\alpha + \gamma\lambda) \quad . \tag{19}$$

Several expressions, a miscellany of experimental information, and some deductions combining experiment and theory all yield values of the coefficients in Eqs (16) and (17). Unfortunately there are many discrepancies and very considerable uncertainties in the experimental data. (Columns 2 through 5 in Table II give weighted estimates for the coefficients, but no great precision is claimed for these values.) One or two points are noteworthy. The approximate constancy of η near 90 km is due to the presence of atomic oxygen; since sunlight is the agency producing the atomic oxygen, this constancy may not be approached at night, although airglow observations indicate an appreciable persistence of atomic oxygen in the upper atmosphere. As height increases, the coefficients α and γ decrease very rapidly at first, but much more slowly above some 40 km; this behavior is the result of three-body processes becoming less important for the greater altitudes.

In order that Eq. (19) can be utilized λ must be determined. A common way of doing this is to assume that the ionic recombination term in Eq. (17) may be neglected, in which case

$$\lambda = \frac{N_-}{N_e} = \frac{\eta}{K} \quad . \tag{20}$$

The assumption implies that $(N_- + N_e)\lambda << K/\gamma$, a quantity which is tabulated in Column 6 of Table II; if the assumption is made, the deduced values of λ and β are those given in Columns 7 and 8. In Column 10, N_e is calculated for values of q indicated by Fig. 1 as being appropriate for the particular heights concerned. Column 11 gives $(N_e + N_-)$ as derived from Columns 7 and 10. If the analysis is self-consistent in supporting the assumption that the ionic recombination term in Eq. (17) can be neglected, then Column 11 should be very much less than Column 6; this is indeed the case over most of the height range being considered, but is only approximately true above some 85 to 90 kilometers.

Table II

h (km)	η	K	γ	α	CONDITION FOR NEGLECTING RECOMBINATION TERM $(N_- + N_e) \ll K/\gamma$ (Quantity Tabulated)	$\lambda = \eta/K$ AS DETERMINED BY NEGLECTING IONIC RECOMBINATION	β USING VALUE IN PREVIOUS COLUMN FOR λ	EXAMPLE OF USE		
								Typical Value of g for h Concerned (Fig. 1)	$N_e = \sqrt{\frac{q}{\beta}}$	$\frac{N_e + N_-}{[N_e (1 + \lambda)]}$
10	8×10^{6}	9×10^{2}	2×10^{-6}	3×10^{-4}	4.5×10^{8}	9×10^{3}	19	10^{2}	2.2	2×10^{4}
20	4×10^{5}	2×10^{2}	6×10^{-7}	10^{-4}	3.3×10^{8}	2×10^{3}	4.4×10^{-1}	10^{8}	1.5×10^{4}	3×10^{7}
30	1×10^{4}	4×10	2×10^{-7}	3×10^{-5}	2×10^{8}	2.5×10^{2}	2.0×10^{-2}	10^{9}	2.2×10^{5}	5.5×10^{7}
40	7×10^{2}	8	7×10^{-8}	10^{-5}	1.1×10^{8}	9×10	1.5×10^{-3}	10^{7}	8.2×10^{4}	7.5×10^{6}
50	5×10	2	6×10^{-8}	4×10^{-6}	3.3×10^{7}	2.5×10	1.4×10^{-4}	10^{6}	8.4×10^{4}	2.2×10^{6}
60	5	7×10^{-1}	5×10^{-8}	2×10^{-6}	1.4×10^{7}	7	1.9×10^{-5}	10^{5}	7.3×10^{4}	5.8×10^{5}
70	3×10^{-1}	2×10^{-1}	5×10^{-8}	10^{-6}	4×10^{6}	1.5	2.7×10^{-6}	10^{4}	6.1×10^{4}	1.5×10^{5}
80	2×10^{-2}	4×10^{-2}	5×10^{-8}	8×10^{-7}	8×10^{5}	0.5	1.2×10^{-6}	10^{3}	2.9×10^{4}	4.3×10^{4}
90	4×10^{-3}	6×10^{-3}	5×10^{-8}	6×10^{-7}	1.2×10^{5}	0.7	1.1×10^{-6}	10^{2}	9.5×10^{3}	1.6×10^{4}
100	4×10^{-3}	8×10^{-4}	5×10^{-8}	4×10^{-7}	1.6×10^{4}	5	3.9×10^{-6}	10	1.6×10^{3}	9.6×10^{3}

By using the values of β given in Table II the contours of q_β plotted on Fig. 1 can readily be converted into contours of N_e. The results obtained are shown in Fig. 2(a). One striking feature of Fig. 2(a) is the bulge in the contours at a height of about 70 km. It is understood that this kind of effect has already been noted by Dr. Cullen M. Crain of RAND Corporation.

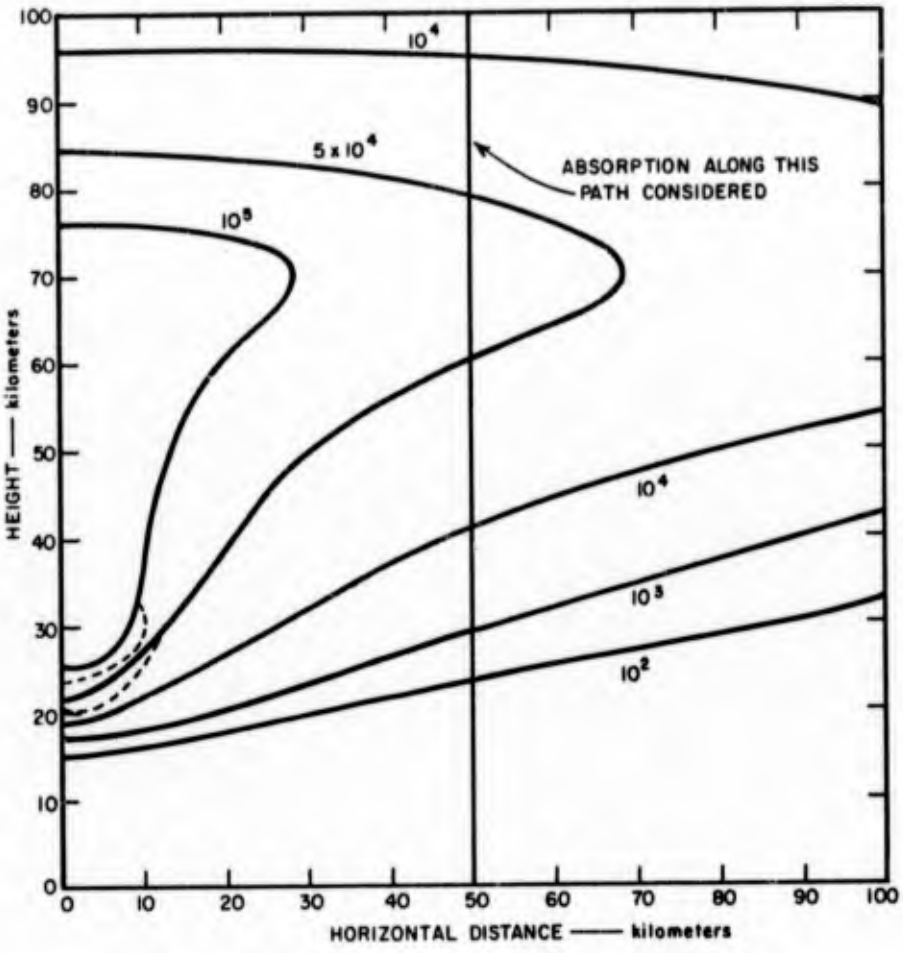

FIG. 2(a)

CONTOURS OF ELECTRON DENSITY (cm^{-3})
(Full curves due to γ radiation alone. Dotted curves--addition due to β radiation)

Figure 2(b) shows the original contours of Fig. 2(a) and a second set obtained using the data of Fig. 1 and the process coefficients given by Crain.[10] In his survey Crain emphasizes our very uncertain knowledge of many of the ionization loss coefficients; the possible discrepancies that can result from these uncertainties are well illustrated on Fig. 2(b).

The second version has less ionization at the lower heights and more at the greater elevations than does the original. Using the second set of contours leads to a modification of the cone of Fig. 6, which is now broader with a base of 1200 km diameter and a depth of 45 km. The two cones are sketched--not to the same horizontal and vertical scales--in an inset on Fig. 2(b).

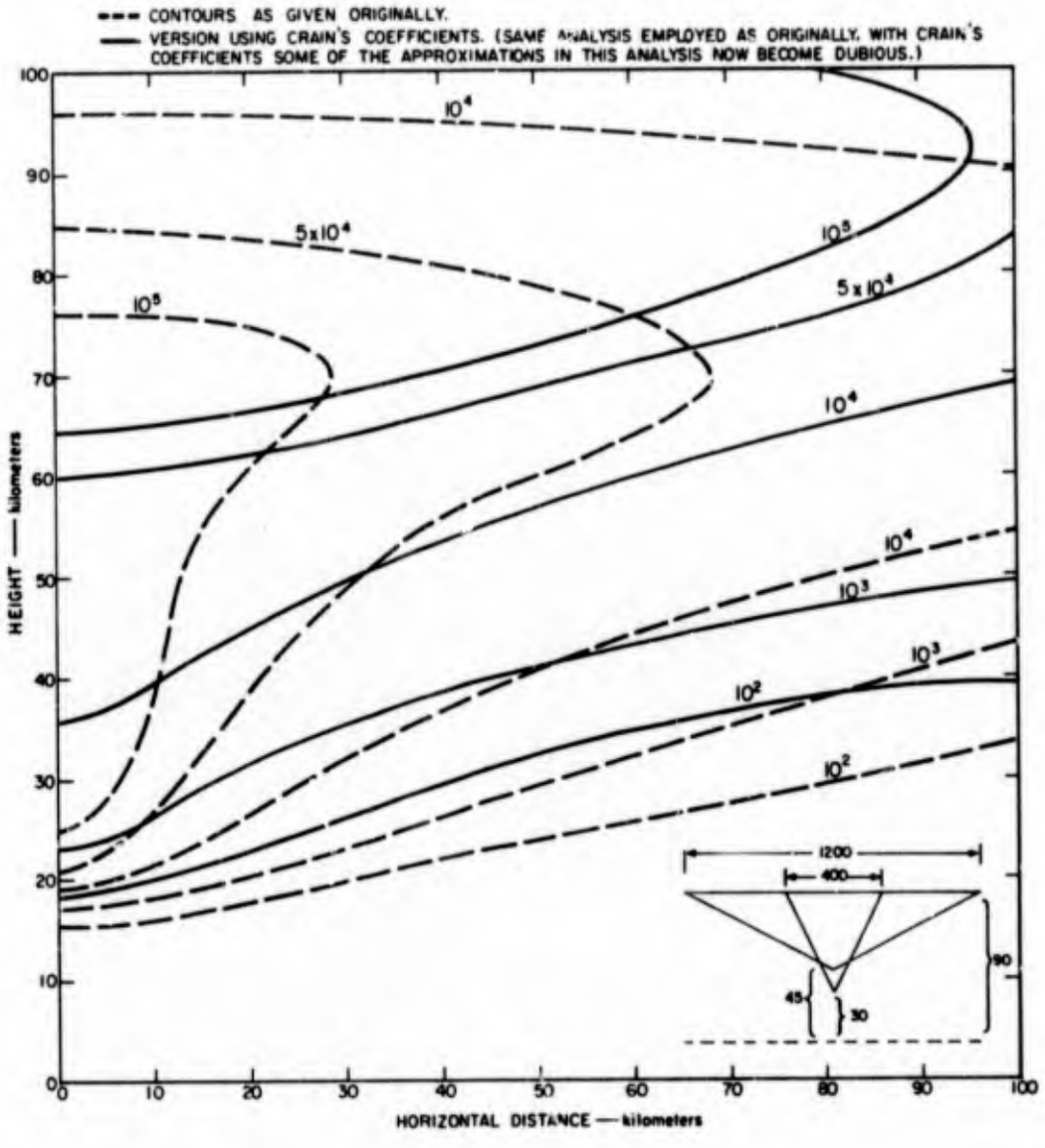

FIG. 2(b)

REVISED CONTOURS OF ELECTRON DENSITY (cm^{-3}) USING CRAIN'S COEFFICIENTS

VI THE EFFECTS ON RADIO PROPAGATION

In the absence of collisions or a magnetic field, a wave of frequency f directed vertically into the ionosphere will be reflected where

$$N_e = 1.24 \times 10^{-8} f^2 \quad . \tag{21}$$

This elementary relation is modified greatly in the full theory, but is still a guide to within an order of magnitude. Accordingly, it may be seen that for electron densities of the order of magnitude of those shown on Fig. 2, most radio frequencies will penetrate the ionization below 100 km, but suffer non-deviative absorption while passing through the region. As frequency is lowered, however, the possibility of reflection at below 100 km becomes increasingly likely. It is therefore instructive to examine the effects of the ionization shown in Fig. 2 for two extreme cases; at a frequency penetrating through the ionosphere and at a very low frequency (VLF) reflected even under normal circumstances from below 100 km. These two ranges of frequencies are important practically. They are also of general significance in studies of ionization below 100 km, since the natural Sudden Ionospheric Disturbance (SID) due to a solar flare, is often detected by the absorption of sources of cosmic noise, or by phase anomalies on VLF propagation.

A. ABSORPTION

If $\omega(=2\pi f)$ is the frequency of the wave being considered and ν is the collisional frequency, then the absorption coefficient, k, may be written as[11]

$$k = 5.3 \times 10^{-3} \left[\frac{N_e \nu}{(\omega^2 + \nu^2)} \right] \tag{22}$$

for the non-deviative absorption in which the refractive index is approximately unity. Suppose that as a specific example the variation of k with height is plotted for f = 18 Mc and the electron vertical profile for a horizontal distance of 50 km, as indicated by Fig. 2. The collisional

frequency values given by Nicolet[12] are taken. The results obtained are shown in Fig. 3. The total absorption below 100 km is about 0.33 neper, which--oddly enough--is also approximately the total absorption of a cosmic noise source, observed from the ground, that is produced by a natural SID. The absorption does not, however, occur at the same height for the two instances; in the case of the natural SID, peak absorption is at near 80 km, but in Fig. 3 the maximum is close to 60 km. Incidentally, 0.33 neper is equal to approximately 2.9 db.

$$E_1 = E_2 \exp(-kz), \quad \ln \frac{E_2}{E_1} = \text{nepers}, \quad 20 \log_{10} \frac{E_2}{E_1} = \text{db} \ .$$

B. VLF PROPAGATION

Very long radio waves are propagated in the waveguide formed by the earth and the lower ionosphere at a height of some 70 km by day and 90 km at night. The electron density at the upper boundary is of the order of $10^2(\text{cm}^{-3})$, and a common approach is to say that this value defines the level of VLF (frequencies from 3-30 kc) reflection. Accordingly, the upper edge of the guide would be taken as defined by the 10^2 contour in Fig. 2. This approach is, however, incorrect. The level of VLF reflection is not determined by electron density alone, but rather by the conductivity and the gradient of conductivity and these involve the collisional frequency as well as the electron density.

In most VLF propagation theory[13] the parameter ω_r which is proportional to the conductivity σ is taken to be characteristic of the upper boundary. Then, with e, m, and ϵ_0 having the conventional significance,

$$\omega_r = \frac{\sigma}{\epsilon_0} = N_e \frac{e^2}{m\epsilon_0} \left(\frac{\nu}{\omega^2 + \nu^2} \right) \approx \frac{N_e}{\nu} \left(\frac{e^2}{m\epsilon_0} \right) \ , \qquad (23)$$

the approximation being certainly valid for a typical VLF ($F \approx 15$ kc) and a height $\leqq 90$ km ($\nu \geq 4.8\ 10^5$). In Fig. 4 contours of ω_r are plotted using the data of Fig. 2 and Nicolet's values for ν. Figure 5 shows for comparison contours of ω_r during normal daytime and night conditions; these contours are, of course, parallel to the ground.

It is well known that the values of ω_r for the homogeneous ionosphere commonly envisaged on the waveguide approach are of the order of 10^4 to 10^6.

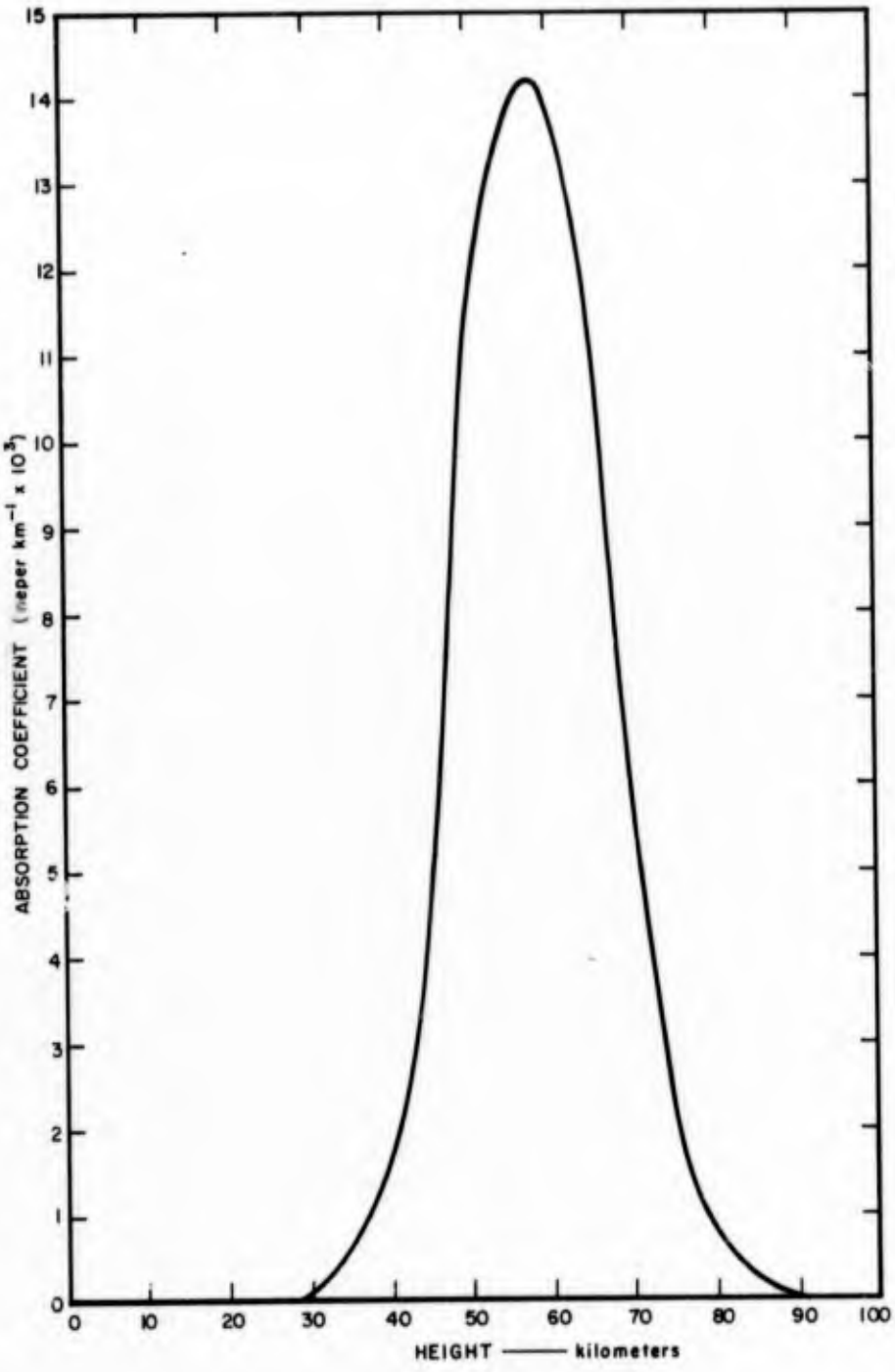

FIG. 3

ABSORPTION AGAINST HEIGHT FOR A FREQUENCY OF 18 Mc

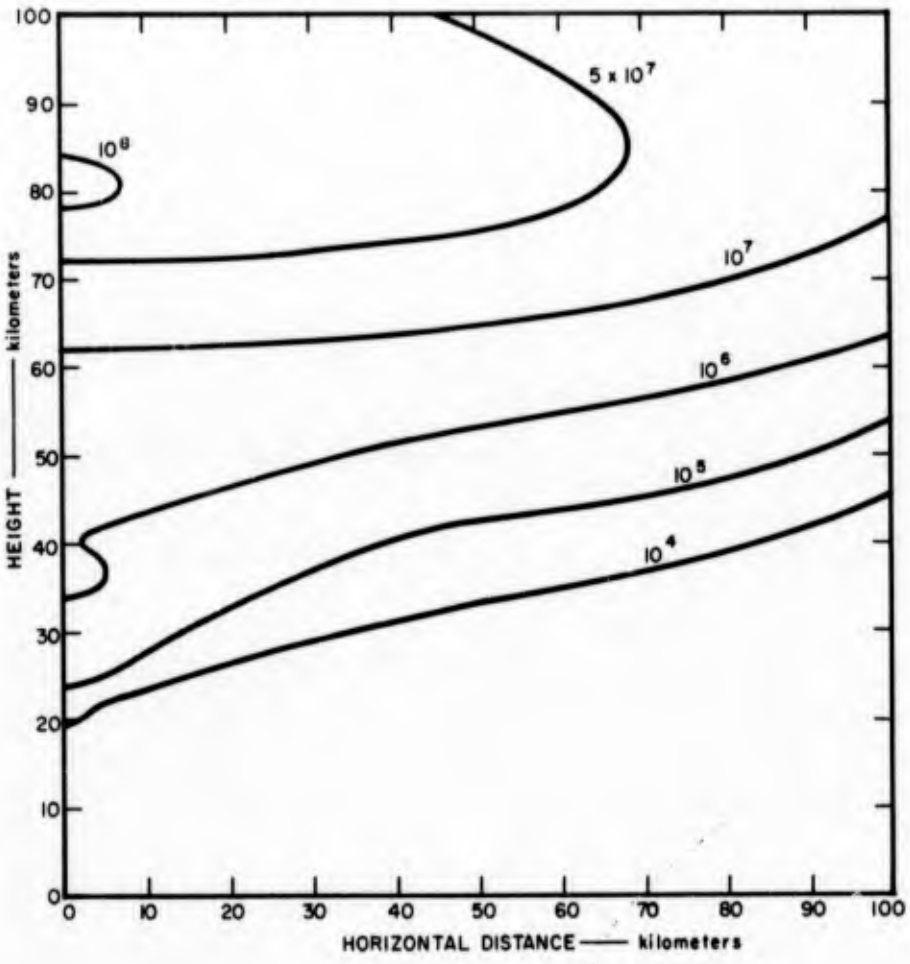

FIG. 4

CONTOURS OF THE PARAMETER ω_r
(Proportional to ionospheric conductivity)

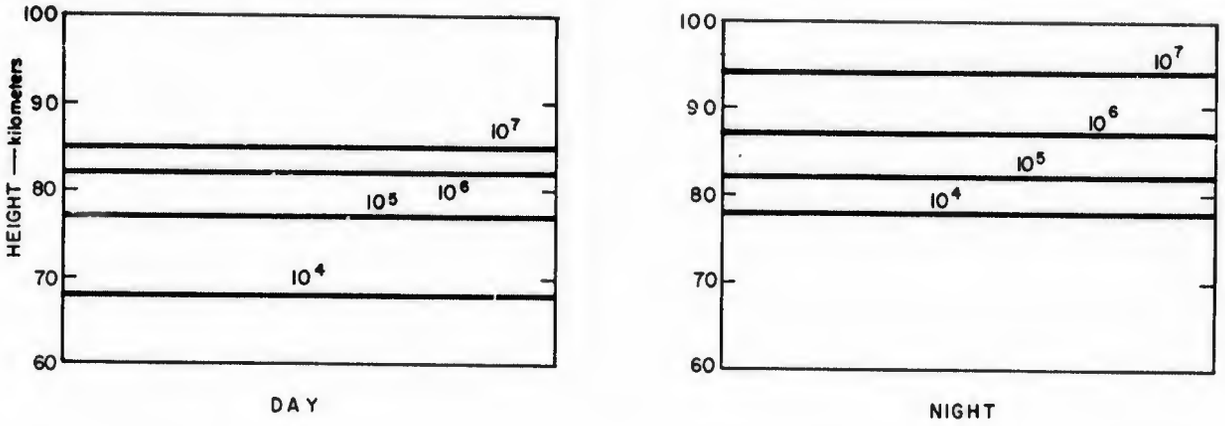

FIG. 5

NORMAL DAY AND NIGHT CONTOURS OF ω_r
(Proportional to ionospheric conductivity)

In actual practice, reflection depends upon the profile of ω_r as well as upon the actual value of ω_r. In Fig. 4 ω_r changes from 10^4 to 10^7 over a distance of some 30 km; in Fig. 5 the corresponding distance is only about 15 km. Thus the gradient of ω_r is approximately twice as steep for the normal conditions of Fig. 5, under which it is known that reflection occurs, as it is for Fig. 4. However, this difference is far less than an order of magnitude and it therefore seems likely that appreciable reflection will take place from the level on Fig. 4 where ω_r is approximately 10^5 to 10^6 in an analogous manner to that usually encountered in conventional VLF propagation

A second approach is to consider the quantity

$$\frac{\lambda_0}{\mu^2}\frac{d\mu}{dh} = C \qquad (24)$$

where λ_0 is the free-space wavelength and μ the refractive index. The greater this quantity the more effective the reflection, and although this criterion is strictly applicable only for short wavelengths, it is at least indicative even for long waves. In the absence of a magnetic field the expression for μ^2 may be written as

$$\mu^2 = \frac{1}{2}\left\{\left[\left(1-\frac{\omega_r}{\nu}\right)^2+\left(\frac{\omega_r}{\omega}\right)^2\right]^{\frac{1}{2}}+1-\frac{\omega_r}{\nu}\right\} ; \qquad (25)$$

$d\mu/dh$ can thus be related to the values of ν, ω_r, $d\omega_r/dh$, and $d\nu/dh$. For normal daytime and night VLF propagation, the quantity C at the reflection level is of the order of unity. Similar values are obtained at the $\omega_r = 10^5$ level in Fig. 4, thus again suggesting that appreciable reflection would occur from this contour.

Figure 6 represents a first approximation to the perturbation of the waveguide produced by the ionization that has been considered. Normal conditions at night are initially envisaged, with VLF propagation being controlled by an ionospheric boundary of height 90 km and with ω_r 10^5 to 10^6. The abnormal ionization produces a boss upon the upper boundary of the guide; this is indicated (in cross section) on Fig. 6 as a shallow cone with apex at height 30 km and a base of 400 km. The boss is considered, in conjunction with the undisturbed guide over 200 km from the central point, to redefine the contour at which $\omega_r = 10^5$ to 10^6.

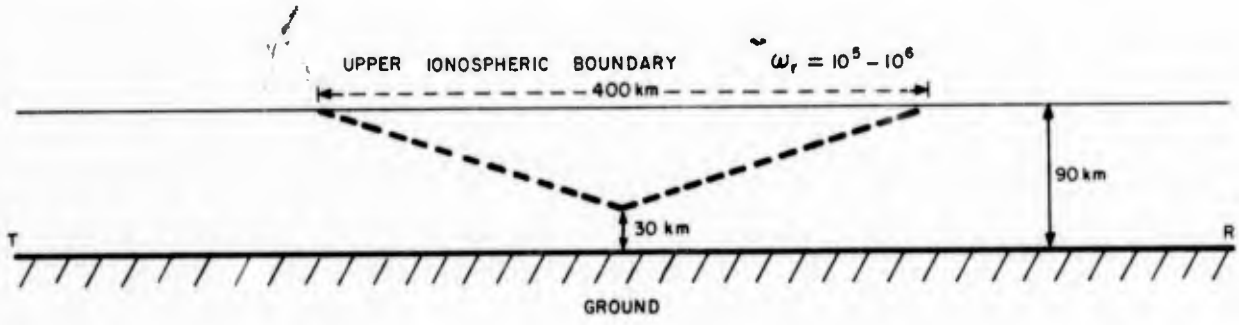

FIG. 6

DISTURBANCE OF THE WAVEGUIDE FOR VLF PROPAGATION AT NIGHT
(Represented by dotted line)

It is difficult to estimate the effects of the indicated perturbation upon VLF propagation between a transmitter T and a receiver R, but it is considered that they would be appreciable. The mathematical complexities involved in modifying the waveguide approach are considerable. When RT is relatively small ($\leq$ 1000 km), it is probably easier to apply a geometric-optic treatment, but the results obtained depend somewhat critically upon the exact characteristics and shape of the boss. Perhaps the easiest way of obtaining approximate information would be to conduct suitably scaled model experiments.

REFERENCES

1. "Effects of Atomic Explosions on Weather," *Atomic Energy*, Vol. 2, No. 2, Science Publication Association, Peking, China (April 1957). Translation from Chinese available as Air Intelligence Information Report 1162011.

2. *Plowshare Series, Part V, Scientific Uses of Nuclear Explosions*, Proceedings of Second Plowshare Symposium at San Francisco, California, 13-15 May 1959; University of California Radiation Laboratory Ref. UCRL 5679.

3. "Report of the Conference of Experts to Study the Possibility of Detecting Violations of a Possible Agreement on the Suspension of Nuclear Tests," United Nations General Assembly Document A/3897 (28 August 1958).

4. W. F. Libby., "Current Research Findings on Radioactive Fallout," *Proc. Natl. Acad. Sci. U.S.*, Vol 42, pp. 945-962 (1956).

5. W. F. Libby., U.S. Atomic Energy Commission, Press release of lecture at University of Washington, March 13, 1959.

6. E. A. Martell, "Atmospheric Aspects of Sr-90 Fallout," *Science*, Vol. 129, pp. 1197-1205 (1959).

7. *Smithsonian Physical Tables*, (Smithsonian Institution, Washington, D.C., ninth revised edition, 1954).

8. R. A. Minzner, K. S. W. Champion and H. L. Pond, "The ARDC Model Atmosphere 1959," Air Force Surveys in Geophysics No. 115, Geophysics Research Directorate, Air Force Cambridge Research Center AFCRC-TR-59-267 (1959).

9. R. Latter and H. Kahn, "Gamma-Ray Absorption Characteristics, Report R-170, RAND Corporation, Santa Monica, California, (1949).

10. C. M. Crain, "Ionization Loss Rates Below 90 Km," *J. Geophys. Res.* 66, pp. 1117-1126 (1961).

11. J. A. Ratcliffe, *The Magneto-Ionic Theory* (Cambridge University Press, Cambridge, England, 1959).

12. M. Nicolet, "The Collision Frequency of Electrons in the Ionosphere," *Phys. Fluids*, Vol. 2, pp. 95-99 (March-April 1959).

13. J. R. Wait, "Terrestial Propagation of Very-Low-Frequency Radio Waves," *J. Research NBS*, Vol. 64D, pp. 153-203 (March-April 1960).